Infectious Disease Modelling 7 (2022) 346–363

Contents lists available at ScienceDirect

Infectious Disease Modelling

journal homepage: www.keaipublishing.com/idm

From pandemic to a new normal: Strategies to optimise governmental interventions in Indonesia based on an SVEIQHR-type mathematical model

Benny Yong*, Jonathan Hoseana, Livia Owen

Center for Mathematics and Society, Department of Mathematics, Parahyangan Catholic University, Bandung, 40141, Indonesia

ARTICLE INFO

Article history:
Received 19 April 2022
Received in revised form 7 June 2022
Accepted 20 June 2022
Available online 30 June 2022
Handling Editor: Dr Lou Yijun

2020 MSC subject classification:
92C60
92D30
34D05

Keywords:
COVID-19
Equilibrium
Basic reproduction number
Intervention
Social restriction
Vaccination

ABSTRACT

There are five different forms of intervention presently realised by the Indonesian government in an effort to end the COVID-19 pandemic: vaccinations, social restrictions, tracings, testings, and treatments. In this paper, we construct a mathematical model of type SVEIQHR (susceptible-vaccinated-exposed-infected-quarantined-hospitalised-recovered) for the disease's spread in the country, which incorporates as parameters the rates of the above interventions, as well as the vaccine's efficacy. We determine the model's equilibria and basic reproduction number. Using the model, we formulate strategies by which the interventions should be realised in order to optimise their impact. The results show that, in a disease-free state, when the number of new cases rises, the best strategy is to implement social restrictions, whereas in an endemic state, if a near-lockdown policy is undesirable, carrying out vaccinations is the best strategy; however, efforts should be aimed not primarily towards increasing the vaccination rate, but towards the use of high-efficacy vaccines.

1. Introduction

Declared to be a pandemic by WHO on March 11, 2020 (Saxena, 2020, page 2), the *coronavirus disease 2019* (COVID-19), reportedly originating from a seafood market in China (Saxena, 2020, page 13–14), has continued to be a global concern, with over 392 million cases recorded worldwide as of February 6, 2022 (WHO, 2022). In most countries, the initial evolution of the daily number of new cases is characterised by several successive waves (Muñoz-Fernández et al., 2021), the end of each wave seemingly indicating successfulness of certain eradicative interventions. Such successfulness was however only temporal in many countries where there occurred subsequent —often larger— waves, of which the emergence of new variants proved to be a principal cause (Page, 2021).

In Indonesia, since mid 2020, amid various disruptions caused by the disease, the government has popularised the term "*a new normal*" to refer to a desired form of post-pandemic life (Adjie, 2020). Its realisability, however, remained unclear. Indeed,

* Corresponding author.
E-mail addresses: benny_y@unpar.ac.id (B. Yong), j.hoseana@unpar.ac.id (J. Hoseana), livia.owen@unpar.ac.id (L. Owen).
Peer review under responsibility of KeAi Communications Co., Ltd.

https://doi.org/10.1016/j.idm.2022.06.004

the largest pre-omicron wave unfolded in mid 2021, the number of new cases reaching a new maximum of 56,767 on July 15, 2021 (Arief, Adji, & Suharto, 2021). The omicron variant then entered the country in late November 2021 (Ranggasari & Bhwana, 2021), before a subsequent wave emerged in January 2022 and the aforementioned maximum was surpassed as early as February 15, 2022, with 57,049 new cases (Rayda, 2022). Keeping the aim towards a new normal, the government of the country has been realising concrete eradicative interventions in the following five different forms.

1. *Vaccinations.* Indonesia's national vaccination programme commenced on January 13, 2021 (Triwadani, 2021), the first vaccinated citizen being the president, Joko Widodo, who received on the day a shot of Coronavac, a vaccine developed by China's Sinovac Biotech, approved for emergency use by the country's Food and Drug Monitoring Agency (BPOM) only two days earlier (Syakriah, 2021). The programme's progress has been tangible: by early 2022, around 45% and 21% of the population have been fully and partially vaccinated, respectively (WHO Indonesia, 2022), and 11 different vaccines with varying levels of efficacy were granted approval (COVID19 Vaccine Tracker). The reception of booster shots has also been urged (Afifa, 2022). Vaccinated citizens are provided with waivers from a number of health-related requirements[1] (Junida, Ihsan, & Suharto, 2022).
2. *Social restrictions.* Besides quarantine regulations for citizens returning from abroad (Indonesia Expat, 2022), the government, in an effort to control the disease's transmission level, has set out four different levels of large-scale social restrictions (PPKM) (Departemen Dalam Negeri, 2021a, 2021b; Saptoyo & Kurniawan, 2021; Double). Each level of social restrictions (1–4) defines a specific degree to which schools, shopping centres, public transport, etc., may operate. At any given time, every region is to implement one of these four restriction levels, carefully determined by the authority based on the region's present situation, using several indicators such as transmission and vaccination levels (Menteri Kesehatan Republik Indonesia, 2021). In particular, responding to the omicron wave, the government has re-raised the levels of social restrictions in various regions including Greater Jakarta, from 2 to 3 (Sucipto, 2022).
3. *Tracings.* Contact tracing, a procedure of interviewing a newly-diagnosed patient with the aim of identifying people who have been in contact with the patient within the last few days (WHO, 2021), has also been in operation, albeit initially at a suboptimal level. (In fact, one of the reasons for the re-raising of the social restrictions level at the start of the omicron wave was the lack of tracings (Sucipto, 2022).) Recently, however, there has been some increase in awareness and government's effort towards contact tracings, as means to break transmission chains (Hutasoit, 2022).
4. *Testings.* Since many COVID-19 patients are asymptomatic, determining whether a person —including travellers and those who have been in recent contact with a patient— is infected is best done via medical testings. At least three types of tests for COVID-19 are available in the country: the polymerase chain reaction test (PCR), the rapid antibody test, and the rapid antigen test (News Desk, 2020).
5. *Treatments.* Being a populous country, Indonesia has faced some considerable difficulty in optimising medical treatments for COVID-19 patients as hospitals became increasingly crowded during the country's largest pre-omicron wave in mid 2021 (WHO Indonesia, 2021). A number of makeshift hospitals were set up, so as to keep the overall bed-occupancy rate within a safe level (WHO Indonesia, 2020). Fortunately, such an effort appeared to be successful in maintaining an acceptable quality of treatment and preventing hospitals from being overwhelmed (Shofa, 2022a). At the start of the omicron wave, the government has, in addition, looked into providing citizens with antiviral medicines, securing 400,000 tablets of molnupiravir (Shofa, 2022b).

In the literature, one finds a large number of studies on the spread of COVID-19, with or without mathematical models, which take into consideration some of the above forms of governmental intervention. In the first place, with regards to vaccinations, studies have confirmed the importance of using high-efficacy vaccines (Dashtbali & Mirzaie, 2021; Moghadas et al., 2021; Sadarangani et al., 2021), starting vaccinations as early as possible (Albani, Loria, Massad, & Zubelli, 2021a, 2021b; Amaku et al., 2021a), and devising vaccination strategies such as age-based prioritisations (Bubar et al., 2021; LimaCampos, Cysne, Madureira, & Mendes, 2021). Some studies have also looked into the necessity of considering the possibility that the number of infection cases is underreported, in the determination of appropriate vaccination strategies (Albani et al., 2021a, 2021b; Gibbons et al., 2014; Lau et al., 2021; Saberi et al., 2020). On the other hand, the impact of social restrictions (Aldila et al., 2020a; Choi & Ki, 2020; Mwalili, Kimathi, Ojiambo, Gathungu, & Mbogo, 2020), as well as that of tracings, testings, and treatments (Alharbi, Alqahtani, Albalawi, & Bakouri, 2020; Amaku et al., 2021b; Aronnaa, Guglielmi, & Moschen, 2021; Chen, Fang, & Huang, 2021 ; Cui, Ni, & Shen, 2021; Gatto & Schellhorn, 2021; Grimm, Mengel, & Schimdt, 2021), have also been a subject of numerous studies. In some of these studies, the employed mathematical models were made more realistic by assuming certain key parameters to be time-dependent, thereby allowing the implementation of parametric fittings which use actual daily data and accommodate fluctuations caused by factors which are not explicitly incorporated to the model (Albani et al., 2021c; Amaku et al., 2021a, 2021b; Aronnaa et al., 2021; Calvetti, Hoover, Rose, & Somersalo, 2020; Cui et al., 2021; LimaCampos et al., 2021).

In (Yong et al., 2022a), we have constructed a SIR-type mathematical model for the spread of COVID-19 in Indonesia, which incorporates —among others— a parameter measuring the aforementioned hospitals' bed-occupancy rate. We have also

[1] There is a true risk of such a policy, which will appear in a later discussion.

Table 1
Parameters used in the model (1) and their values chosen for our numerical simulations (section 3).

Parameter	Description	Unit	Value for simulation	Source
λ	recruitment rate of newborns	individual/day	$\frac{273523621}{65 \times 365}$	estimated as $\mu N(0)$ World Bank (2020)
λ'	recruitment rate of foreigners	individual/day	3000	Indonesia Expat (2021)
μ	natural death rate	1/day	$\frac{1}{65 \times 365}$	Aldila, Samiadji, Simorangkir, Khosnaw, and Shahzad (2021)
μ'	death rate increment due to COVID-19	1/day	0.0291	Gugus Tugas Percepatan Penanganan COVID
β	transmission coefficient	1/(individual $\times$ day)	4.74396×10^{-8}	Aldila et al. (2021)
δ	vaccine efficacy	dimensionless	see subsection 3.1	
α	temporary immunity rate	1/day	0.011	Shakhany and Salimifard (2021)
θ	incubation rate	1/day	0.4	Prem et al. (2020)
γ	recovery rate of infected individuals	1/day	0.1	Ferguson et al. (2020)
φ	recovery rate of hospitalised individuals	1/day	0.8198	Gugus Tugas Percepatan Penanganan COVID
κ	recovery rate of quarantined individuals	1/day	0.1	Ferguson et al. (2020)
τ	hospitalisation rate of quarantined individuals	1/day	0.01	Aldila et al. (2020b)
u_1	vaccination rate	1/day	0.4	Diagne, Rwezaura, Tchoumi, and Tchuenche (2021)
u_2	mobility intervention rate	dimensionless	see subsection 3.1	
u_3	contact-tracing intervention rate	1/day	0.5	assumed
u_4	rapid-testing intervention rate	1/day	0.3	assumed
u_5	treatment intervention rate	1/day	0.0833	Babaei, Jafari, Banihashemi, and Ahmadi (2021)

constructed a discrete version of this model, in which some parameters were assumed to be time-dependent, and use it to design a quantitative method for determining the appropriate level(s) of social restrictions to be enforced in Jakarta on any given day (Yong et al., 2022b). In this paper, taking into consideration the above five forms of intervention, as well as the idea proposed in (Mu ñ oz-Fern á ndez et al., 2021, section 4) of incorporating more compartments and the possibility of reinfection, we aim to construct a new model which is more comprehensive and realistic, with the hope of formulating strategies by which the above forms of intervention should be realised in order to optimise their impact, so that a new normal can be embraced as soon as possible.

The incorporation of additional compartments implies that the present model is no longer SIR-type. Indeed, we shall take into account, at any given time $t \geqslant 0$, the numbers $S = S(t)$ of (unvaccinated) *susceptible* individuals, $V = V(t)$ of (susceptible) *vaccinated* individuals, $E = E(t)$ of (non-transmitting) *exposed* individuals, $I = I(t)$ of *infected* individuals, $Q = Q(t)$ of *quarantined* individuals, $H = H(t)$ of *hospitalised* individuals, and $R = R(t)$ of *recovered* individuals, thereby building a seven-compartment SVEIQHR-type model. We assume that all quarantines are centralised, so that the quarantined —as well as the hospitalised— individuals are never in contact with the susceptible and vaccinated individuals, meaning that only the infected individuals transmit the disease. We also assume that social restrictions are waived for vaccinated citizens[2]; see, e.g., (Junida, Ihsan, & Suharto, 2022). The above five forms of intervention shall be incorporated to the model as parameters u_1, u_2, u_3, u_4, and u_5, all belonging to [0, 1], which represent, respectively, the rates of vaccine, mobility, contact-tracing, rapid-testing, and treatment interventions.[3] We shall also incorporate a parameter $\delta \in [0, 1]$ representing the vaccine efficacy. These and all other parameters, together with their values used in our numerical analysis, are described in Table 1.

Let us now construct the model itself, by detailing the changes assumed to be experienced at any given time by each of the above seven time-dependent variables, which are summarised in the compartment diagram in Fig. 1.

1. The number S of susceptible individuals increases due to the entry of newborns at the rate $\lambda > 0$ and of recovered individuals at the rate αR, where $\alpha > 0$, and decreases due to the exit of those who become exposed at the rate $(1 - u_2)\beta SI$, where $u_2 \in [0, 1]$ and $\beta > 0$, vaccinated at the rate $u_1 S$, where $u_1 \in [0, 1]$, and dead at the rate μS, where $\mu > 0$.
2. The number V of vaccinated individuals increases due to the entry of susceptible individuals at the rate $u_1 S$, and decreases due to the exit of those who become exposed at the rate $(1 - \delta)\beta VI$, where $\delta \in [0, 1]$, and dead at the rate μV. Notice that the

[2] This could be an imprudent policy; see subsection 3.1.
[3] Thus, $u_2 = 0$ represents normal mobility, while $u_2 = 1$ represents a total lockdown. For a method to estimate the value of u_2 representing each of the four levels of social restrictions, see subsection 3.1.

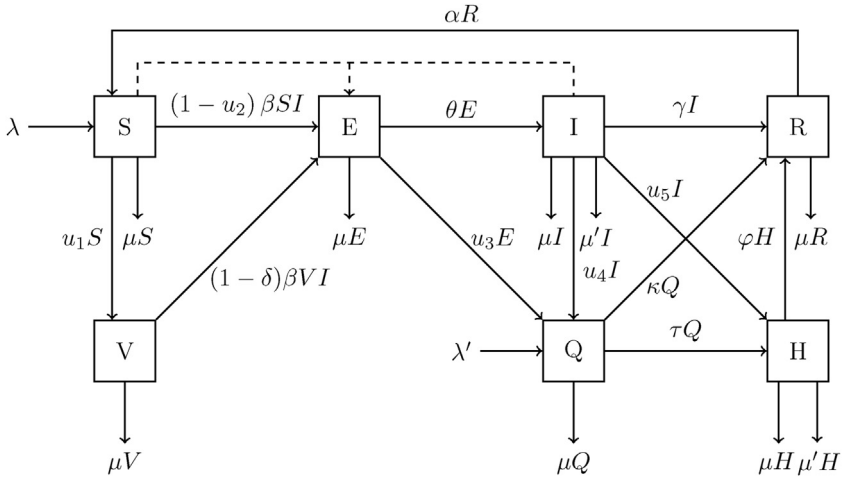

Fig. 1. The compartment diagram of our SVEIQHR-type model.

former does not contain the mobility restriction factor $1-u_2$ as in the rate at which susceptible individuals become exposed; this manifests our assumption that social restrictions are waived for vaccinated citizens.

3. The number E of exposed individuals increase due to the entry of susceptible individuals at the rate $(1-u_2)\beta SI$ and of vaccinated individuals at the rate $(1-\delta)\beta VI$, and decreases due to the exit of those who become infected at the rate θE, where $\theta > 0$, quarantined at the rate $u_3 E$, where $u_3 \in [0,1]$, and dead at the rate μE.
4. The number I of infected individuals increase due to the entry of exposed individuals at the rate θE, and decreases due to the exit of those who become recovered at the rate γI, where $\gamma > 0$, quarantined at the rate $u_4 I$, where $u_4 \in [0,1]$, hospitalised at the rate $u_5 I$, where $u_5 \in [0,1]$, and dead at the rate $(\mu+\mu')I$, where $\mu' > 0$.
5. The number Q of quarantined individuals increase due to the entry of foreigners at the rate $\lambda' > 0$, of exposed individuals at the rate $u_3 E$, and of infected individuals at the rate $u_4 I$, and decreases due to the exit of those who become recovered at the rate κQ, where $\kappa > 0$, hospitalised at the rate τQ, where $\tau > 0$, and dead at the rate μQ.
6. The number H of hospitalised individuals increase due to the entry of quarantined individuals at the rate κQ and of infected individuals at the rate $u_5 I$, and decreases due to the exit of those who become recovered at the rate φH, where $\varphi > 0$, and dead at the rate $(\mu+\mu')H$.
7. The number R of recovered individuals increases due to the entry of infected individuals at the rate γI, quarantined individuals at the rate κQ, and hospitalised individuals at the rate φH, and decreases due to the exit of those who become susceptible at the rate αR and dead at the rate μR.

We therefore obtain the model

$$
\begin{cases}
\dfrac{\mathrm{d}S}{\mathrm{d}t} &= \lambda + \alpha R - (1-u_2)\beta SI - u_1 S - \mu S,\\
\dfrac{\mathrm{d}V}{\mathrm{d}t} &= u_1 S - (1-\delta)\beta VI - \mu V,\\
\dfrac{\mathrm{d}E}{\mathrm{d}t} &= (1-u_2)\beta SI - \theta E + (1-\delta)\beta VI - u_3 E - \mu E,\\
\dfrac{\mathrm{d}I}{\mathrm{d}t} &= \theta E - \gamma I - u_4 I - u_5 I - \mu I - \mu' I,\\
\dfrac{\mathrm{d}Q}{\mathrm{d}t} &= \lambda' + u_3 E + u_4 I - \kappa Q - \tau Q - \mu Q,\\
\dfrac{\mathrm{d}H}{\mathrm{d}t} &= \tau Q + u_5 I - \varphi H - \mu H - \mu' H,\\
\dfrac{\mathrm{d}R}{\mathrm{d}t} &= \gamma I - \alpha R + \kappa Q + \varphi H - \mu R.
\end{cases}
\tag{1}
$$

The rest of the paper is organised as follows. In the upcoming section 2, we analyse the model (1) dynamically. We first establish the non-negativity and boundedness of its solutions, and determine a subdomain which is positively invariant under the model (subsection 2.1). Next, we show that, for every set of parameter values, the model possesses a unique disease-free

equilibrium, and determine an explicit expression of this equilibrium (subsection 2.2). We also derive the model's basic reproduction number $\mathcal{R}_0$ and show that, if $\mathcal{R}_0 < 1$, the disease-free equilibrium is stable, whereas if $\mathcal{R}_0 > 1$, the disease-free equilibrium is unstable and a unique positive endemic equilibrium exists (subsections 2.2 and 2.3).

As the algebraic computations required to establish further dynamical properties of the model —such as the endemic equilibrium's stability— appear to be inaccessibly complicated, we shift from analytical to numerical methods (section 3), whose flexibility allows us to achieve our ultimate goal: formulating strategies by which the aforementioned forms of governmental intervention (vaccinations, social restrictions, tracings, testings, and treatments) should be implemented for an optimal impact. The first stage of our analysis yields results which strongly point towards vaccinations, and more specifically, towards the importance of a high vaccine efficacy, in addition to the necessity of unwaiving social restrictions for vaccinated citizens (subsection 3.1). This is confirmed quantitatively in our second stage (subsection 3.2) via sensitivity analysis, from which we conclude that the optimal intervention strategy is to implement social restrictions in the case of $\mathcal{R}_0 < 1$, and, if a lockdown is undesirable, vaccinations using high-efficacy vaccines in the case of $\mathcal{R}_0 > 1$. These conclusions are reasserted in section 4, where we also describe a number of ways in which the model (1) could be modified for further research.

2. Dynamical analysis

Let us first analyse the model (1) from the viewpoint of dynamical systems theory; see (Martcheva, 2015; Robinson, 2012) for background. First, we establish the non-negativity and boundedness of the model's solutions associated to non-negative initial conditions, and the positive-invariance of a bounded subdomain (Theorem 1). Subsequently, we show that the model has a unique disease-free equilibrium for every set of parameter values, which is stable if $\mathcal{R}_0 < 1$ and unstable if $\mathcal{R}_0 > 1$, where $\mathcal{R}_0$ is the model's basic reproduction number (Theorem 2). Finally, we show that in the case of $\mathcal{R}_0 > 1$, in which the model's solutions do not approach the disease-free equilibrium, a unique positive endemic equilibrium exists (Theorem 3).

2.1. Non-negativity and boundedness of solutions

Let us first establish the non-negativity and boundedness of the solutions of the model (1) associated to non-negative initial conditions. Let

$$(S(0), V(0), E(0), I(0), Q(0), H(0), R(0)) \in \mathbb{R}_+^7$$

be such an initial condition, where $\mathbb{R}_+ := [0, \infty)$, and let $(S(t), V(t), E(t), I(t), Q(t), H(t), R(t))$ be the solution associated to this initial condition. For every $t^* \geqslant 0$ satisfying $S(t^*) = 0$, we have, from the model's first equation,

$$\left.\frac{\mathrm{d}S}{\mathrm{d}t}\right|_{t=t^*} = \lambda + \alpha R(t^*) > 0,$$

which means that the function S is increasing at t^*. Since $S(0) \geqslant 0$, it follows that $S(t) \geqslant 0$ for every $t \geqslant 0$. Similar arguments show that

$$V(t) \geqslant 0, \quad E(t) \geqslant 0, \quad I(t) \geqslant 0, \quad Q(t) \geqslant 0, \quad H(t) \geqslant 0, \quad \text{and} \quad R(t) \geqslant 0$$

for every $t \geqslant 0$.

Next, adding all equations in (1), one obtains that the time-dependent total population $N := S + V + E + I + Q + H + R$ satisfies

$$\frac{\mathrm{d}N(t)}{\mathrm{d}t} \leqslant \lambda + \lambda' - \mu N(t),$$

which is equivalent to

$$\frac{\mathrm{d}}{\mathrm{d}t}\left(N(t)\mathrm{e}^{\mu t}\right) \leqslant \frac{\mathrm{d}}{\mathrm{d}t}\left(\frac{\lambda + \lambda'}{\mu}\mathrm{e}^{\mu t} + N(0) - \frac{\lambda + \lambda'}{\mu}\right). \tag{2}$$

Now, the functions $N(t)\mathrm{e}^{\mu t}$ and $((\lambda + \lambda')/\mu)\mathrm{e}^{\mu t} + N(0) - (\lambda + \lambda')/\mu$ have the same value at $t = 0$, namely, $N(0)$, and, by (2), at every point, the slope of the former function does not exceed that of the latter function. Consequently, for every $t \geqslant 0$ we have

$$N(t)\mathrm{e}^{\mu t} \leqslant \frac{\lambda + \lambda'}{\mu}\mathrm{e}^{\mu t} + N(0) - \frac{\lambda + \lambda'}{\mu},$$

i.e.,

$$N(t) \leqslant \frac{\lambda+\lambda'}{\mu} + \left(N(0) - \frac{\lambda+\lambda'}{\mu}\right) e^{-\mu t} \overset{t\to\infty}{\to} \frac{\lambda+\lambda'}{\mu}.$$

This implies that the solution $(S(t), V(t), E(t), I(t), Q(t), H(t), R(t))$ is bounded, and that the subset

$$\mathcal{D} := \left\{ \left(S, V, E, I, Q, H, R\right) \in \mathbb{R}^7_+ : S + V + E + I + Q + H + R \leqslant \frac{\lambda+\lambda'}{\mu} \right\} \subseteq \mathbb{R}^7_+$$

is positively invariant (60, Definition 4.4) under the model.

We summarise our results in the following theorem.

Theorem 1. (1) *Every solution of the model* (1) *associated to an initial condition in* $\mathbb{R}^7_+$ *is bounded and remains forever in* $\mathbb{R}^7_+$.
(2) *Every solution of the model* (1) *associated to an initial condition in* $\mathcal{D}$ *remains forever in* $\mathcal{D}$.

2.2. Disease-free equilibrium and basic reproduction number

Let us now study the equilibria of the model (1), i.e., the solutions of the system

$$\begin{cases} \lambda + \alpha R - (1-u_2)\beta SI - u_1 S - \mu S &= 0, \\ u_1 S - (1-\delta)\beta VI - \mu V &= 0, \\ (1-u_2)\beta SI - \theta E + (1-\delta)\beta VI - u_3 E - \mu E &= 0, \\ \theta E - \gamma I - u_4 I - u_5 I - \mu I - \mu' I &= 0, \\ \lambda' + u_3 E + u_4 I - \kappa Q - \tau Q - \mu Q &= 0, \\ \tau Q + u_5 I - \varphi H - \mu H - \mu' H &= 0, \\ \gamma I - \alpha R + \kappa Q + \varphi H - \mu R &= 0. \end{cases} \tag{3}$$

We shall begin by showing that, for every set of parameter values, the model possesses a unique disease-free equilibrium, which admits an explicit description, and relating its stability to the model's basic reproduction number.

Let $\mathbf{e}_0 = (S_0, V_0, E_0, I_0, Q_0, H_0, R_0)$ be a disease-free equilibrium of the model (1), i.e., a solution of (3) satisfying $I_0 = 0$. The fourth equation in (3) gives $E_0 = 0$. The fifth, sixth, seventh, first, and second equations then give, respectively, Q_0, H_0, R_0, S_0, and V_0. In explicit form,

$$S_0 = k_6, \quad V_0 = \frac{u_1 k_6}{\mu}, \quad E_0 = 0, \quad I_0 = 0, \quad Q_0 = \frac{\lambda'}{k_3}, \quad H_0 = \frac{\tau\lambda'}{k_3 k_4}, \quad R_0 = \frac{\lambda'(\kappa k_4 + \varphi\tau)}{k_3 k_4 k_5},$$

where

$$\begin{aligned} &k_1 = \theta + u_3 + \mu, \quad k_2 = \gamma + u_4 + u_5 + \mu + \mu', \quad k_3 = \kappa + \tau + \mu, \quad k_4 = \varphi + \mu + \mu', \\ &k_5 = \mu + \alpha, \quad \text{and} \quad k_6 = \frac{\lambda}{u_1 + \mu} + \frac{\alpha\lambda'\kappa}{(u_1+\mu)k_3 k_5} + \frac{\alpha\lambda'\varphi\tau}{(u_1+\mu)k_3 k_4 k_5}. \end{aligned} \tag{4}$$

The disease-free equilibrium $\mathbf{e}_0$ thus exists —since all its components are positive— and is unique, for every set of parameter values.

Let us now compute the model's basic reproduction number, using the so-called *next-generation matrix method* (van den Driessche & Watmough, 2002, page 33), taking into account as infected compartments those of exposed, infected, quarantined, and hospitalised individuals, whose numbers evolve at the rates given by the third, fourth, fifth, and sixth equations of the model (1). Letting $(X_1, X_2, X_3, X_4) := (E, I, Q, H)$, we first define

$$\mathcal{F}_1 := (1-u_2)\beta S X_2 + (1-\delta)\beta V X_2, \quad \mathcal{F}_2 := 0, \quad \mathcal{F}_3 := 0, \quad \mathcal{F}_4 := 0,$$

and

$$\begin{aligned} \mathcal{V}_1 &:= \theta X_1 + u_1 X_1 + \mu X_1, \\ \mathcal{V}_2 &:= -\theta X_1 + \gamma X_2 + u_4 X_2 + u_5 X_2 + \mu X_2 + \mu' X_2, \\ \mathcal{V}_3 &:= -\lambda' - u_3 X_1 - u_4 X_2 + \kappa X_3 + \tau X_3 + \mu X_3, \\ \mathcal{V}_4 &:= -\tau X_3 - u_5 X_2 + \varphi X_4 + \mu X_4 + \mu' X_4. \end{aligned}$$

Next, we define the 4×4 matrices

$$\mathbf{F} := \left(\frac{\partial \mathcal{F}_i}{\partial X_j}(\mathbf{e}_0)\right) = \begin{pmatrix} 0 & (1-u_2)\beta k_6 + (1-\delta)\beta u_1 k_6/\mu & 0 & 0 \\ 0 & 0 & 0 & 0 \\ 0 & 0 & 0 & 0 \\ 0 & 0 & 0 & 0 \end{pmatrix}.$$

and

$$\mathbf{V} := \left(\frac{\partial \mathcal{V}_i}{\partial X_j}(\mathbf{e}_0)\right) = \begin{pmatrix} k_1 & 0 & 0 & 0 \\ -\theta & k_2 & 0 & 0 \\ -u_3 & -u_4 & k_3 & 0 \\ 0 & -u_5 & -\tau & k_4 \end{pmatrix}.$$

The basic reproduction number of the model (1) is the spectral radius of the model's next-generation matrix $\mathbf{F}\mathbf{V}^{-1}$:

$$\mathcal{R}_0 := \rho\left(\mathbf{F}\mathbf{V}^{-1}\right) = \frac{\theta\beta k_6(\mu(1-u_2)+(1-\delta)u_1)}{k_1 k_2 \mu}. \tag{5}$$

Therefore, the basic reproduction number $\mathcal{R}_0$ grows only sublinearly with the vaccination rate u_1. This means that, for the eradication of COVID-19, it is not advisable to strive *only* towards a high vaccination rate; indeed, many of the countries with high percentages of citizens vaccinated (Wolf et al., 2022) retain their pandemic status. Instead, since $\mathcal{R}_0$ grows linearly with the mobility intervention rate u_2, and with the vaccine efficacy δ, these parameters deserve more attention. In subsection 3.2, we shall confirm quantitatively that this is the case, i.e., that these are the parameters upon which $\mathcal{R}_0$ depends most sensitively in the cases of $\mathcal{R}_0 < 1$ and $\mathcal{R}_0 > 1$, respectively.

Direct computation shows that the characteristic polynomial of the Jacobian matrix of the model (1) evaluated at $\mathbf{e}_0$ is given by

$$P(x) = (x+\mu)(x+u_1+\mu)(x+k_3)(x+k_4)(x+k_5)\left(x^2+bx+c\right),$$

where

$$\begin{aligned} b &:= 2\mu+\gamma+\theta+u_3+u_4+u_5+\mu', \\ c &:= \mu^2+(\gamma+\theta+u_3+u_4+u_5+\mu')\mu+((u_2-1)\beta k_6+\gamma+u_4+u_5+\mu')\theta \\ &\quad +u_3(\gamma+u_4+u_5+\mu')+\frac{\beta\theta k_6 u_1(\delta-1)}{\mu}, \end{aligned}$$

meaning that $-\mu$, $-u_1-\mu$, $-k_3$, $-k_4$, and $-k_5$ are five negative roots of $P(x)$. Therefore, the equilibrium $\mathbf{e}_0$ is locally asymptotically stable if the other two roots x_1 and x_2, i.e., those of x^2+bx+c, have negative real parts (Robinson, 2012, Theorem 4.6(a)), and is unstable if at least one of x_1 and x_2 have a positive real part. Since $b>0$, the former holds if $c>0$ (by the Routh-Hurwitz criterion (Allen, 2007, section 4.5)), while the latter holds if $c<0$ (in which case x_1 and x_2 are real and have opposite signs). Direct computation shows that $c>0$ is equivalent to $\mathcal{R}_0<1$, while $c<0$ is equivalent to $\mathcal{R}_0>1$. This proves the following theorem.

Theorem 2. *For every set of parameter values, the model* (1) *has a unique disease-free equilibrium, which is locally asymptotically stable if* $\mathcal{R}_0<1$, *and unstable if* $\mathcal{R}_0>1$.

2.3. Endemic equilibria

Let us now seek all equilibria $\mathbf{e}_n = (S_n, V_n, E_n, I_n, Q_n, H_n, R_n)$ with $I_n \neq 0$, $n \in \mathbb{N}$. First, solving the fifth equation in (3) for Q_n gives

$$Q_n = \frac{\lambda' + u_3 E_n + u_4 I_n}{k_3}. \tag{6}$$

Substituting (6) into the sixth equation in (3) and solving the resulting equation for H_n gives

$$H_n = \frac{1}{k_4}\left(\frac{\tau}{k_3}(\lambda' + u_3 E_n + u_4 I_n) + u_5 I_n\right). \tag{7}$$

Next, substituting (6) and (7) into the seventh equation in (3) and solving the resulting equation for R_n gives

$$R_n = \frac{1}{k_5}\left(\gamma I_n + \frac{\kappa}{k_3}(\lambda' + u_3E_n + u_4I_n) + \frac{\varphi}{k_4}\left(\frac{\tau}{k_3}(\lambda' + u_3E_n + u_4I_n) + u_5I_n\right)\right), \tag{8}$$

Subsequently, substituting (8) into the first equation in (3) and solving the resulting equation for S_n gives

$$S_n = \frac{1}{\mu + u_1 + (1-u_2)\beta I_n}\left(\lambda + \frac{\alpha}{k_5}\left(\gamma I_n + \frac{\kappa}{k_3}(\lambda' + u_3E_n + u_4I_n) + \frac{\varphi}{k_4}\left(\frac{\tau}{k_3}(\lambda' + u_3E_n + u_4I_n) + u_5I_n\right)\right)\right) \tag{9}$$

In addition, substituting (9) into the second equation in (3) and solving the resulting equation for V_n gives

$$V_n = \frac{u_1S_n}{(1-\delta)\beta I_n + \mu}. \tag{10}$$

Solving the third and fourth equations in (3) for E_n gives, respectively,

$$E_n = \frac{1}{k_1}((1-u_2)\beta S_nI_n + (1-\delta)\beta V_nI_n) \quad \text{and} \quad E_n = \frac{k_2I_n}{\theta}. \tag{11}$$

Equating the two equations in (11) yields

$$V_n = \frac{\beta\theta u_2S_n - \beta\theta S_n + k_1k_2}{\theta(1-\delta)\beta}.$$

Equating this and (10) yields the following expression of S_n as a function of I_n:

$$S_n = \frac{k_1k_2(\mu + \beta I_n - \beta\delta I_n)}{\beta\theta(\beta\delta u_2I_n - \beta\delta I_n - \beta u_2I_n + \beta I_n - u_1\delta - \mu u_2 + \mu + u_1)}. \tag{12}$$

On the other hand, substituting the second equation in (11) and into (9) yields another expression of S_n as a function of I_n:

$$S_n = \frac{1}{\mu + u_1 + (1-u_2)\beta I_n}\left(\lambda + \frac{\alpha}{k_5}\left(\gamma I_n + \frac{\kappa}{k_3}\left(\lambda' + \frac{k_2u_3I_n}{\theta} + u_4I_n\right) + \frac{\varphi}{k_4}\left(\frac{\tau}{k_3}\left(\lambda' + \frac{k_2u_3I_n}{\theta} + u_4I_n\right) + u_5I_n\right)\right)\right). \tag{13}$$

Equating (12) and (13), one finds that the values of I_n are the roots of the quadratic polynomial

$$dI_n^2 + eI_n + f, \tag{14}$$

where

$$\begin{aligned}
d &:= (1-\delta)\theta(1-u_2)\beta^2((((\gamma k_3 + \kappa u_4)k_4 + \varphi(k_3u_5 + \tau u_4))\theta + u_3k_2(k_4\kappa + \tau\varphi))\alpha \\
&\quad - k_1k_2k_3k_4k_5),\\
e &:= \theta((((\gamma((1-u_2)\mu + u_1(1-\delta)))k_3 - (u_4(u_2-1)\mu + (u_1u_4 - \beta\lambda'(u_2-1))(\delta-1))\kappa)k_4 \\
&\quad - \varphi(u_5((u_2-1)\mu + u_1(\delta-1)))k_3 + \tau(u_4(u_2-1)\mu + (u_1u_4 - \beta\lambda'(u_2-1))(\delta-1))))\theta \\
&\quad - u_3k_2(k_4\kappa + \tau\varphi)((u_2-1)\mu + u_1(\delta-1)))\alpha + k_3k_4k_5(\beta\lambda(u_2-1)(\delta-1)\theta \\
&\quad + ((\delta - u_2 - 2)\mu + u_1(\delta-1))k_1k_2))\beta,\\
f &:= \theta(((1-u_2)\mu + u_1(1-\delta))((\alpha\kappa\lambda' + k_3k_5\lambda)k_4 + \alpha\varphi\lambda'\tau)\beta\theta - k_1k_2k_3k_4k_5\mu(\mu + u_1)).
\end{aligned}$$

Direct computation shows that the condition $\mathcal{R}_0 > 1$ is equivalent to $f/d < 0$. If this holds, then the values of I_n are real (since $fd < 0$) and have opposite signs: $I_1 > 0$ and $I_2 < 0$, say. Substituting I_1 into (6), (7), (8), (9), (10), and (11), one obtains a unique endemic equilibrium $\mathbf{e}_1 = (S_1, V_1, E_1, I_1, Q_1, H_1, R_1)$ of the model (1), with all components positive. We have therefore proved the following theorem.

Theorem 3. *If $\mathcal{R}_0 > 1$, then the model (1) has a unique positive endemic equilibrium.*

In the case of $\mathcal{R}_0 < 1$, we have $f/d > 0$, and so no immediate conclusion can be drawn on whether the values of I_n are real. Obtaining an analytic expression for the polynomial's discriminant $e^2 - 4df$ requires tedious computations, let alone examining its non-negativity. The same situation is faced as we attempt to characterise the stability of these endemic equilibria in the case of their existence, since the analytic expression of I_n given by the quadratic formula is already complicated. This forces us to migrate from analytical to numerical techniques. Preliminary numerical experiments show that, for the parameter values shown in Table 1, $\delta = 0.653$, $u_1 = 10^{-8}$, and $u_2 = 0.93$, in which case $\mathcal{R}_0$ is less than but very close to 1 (cf. first case in subsection 3.2), the polynomial

(14) *has two negative real roots, suggesting that the bifurcation occurring at* $\mathcal{R}_0 = 1$ *is a forward transcritical bifurcation* (Dashtbali and Mirzaie, 2021, subsection 3.4.3). *Subsequently, replacing* u_1 *and* u_2 *with* 0.4 *and* 0.278, *respectively, we observe that* $\mathcal{R}_0$ *is greater than* 1 (*cf. second case in* subsection 3.2) *and that a solution of the model* (1) *converges towards the unique positive endemic equilibrium guaranteed to exist by* Theorem 3 (*cf. red graph in* Fig. 7), *suggesting that this equilibrium is stable in the case of its existence*.

3. Formulation of intervention strategies

We have mentioned the five concrete forms of intervention presently realised by the Indonesian government to strive towards a new normal: vaccinations, social restrictions, tracings, testings, and treatments. Now, we are ready to exploit the model (1) to formulate strategies for realising these forms of intervention, in order to optimise their impact. This will be achieved via a two-stage analysis —which is both numerical and interpretative— of the model's basic reproduction number $\mathcal{R}_0$. The first stage is the preliminary analysis, where we identify the set of parameter values corresponding to the *disease-free region* —that in which $\mathcal{R}_0 < 1$— and its realisability, in various epidemic scenarios. The results, as we shall see, point towards the necessity of vaccinations, and, more importantly, the vaccine efficacy, as important keys to achieve a new normal. The second stage consists in an analysis of the sensitivity of $\mathcal{R}_0$ with respect to each parameter. For each of the two cases $\mathcal{R}_0 < 1$ and $\mathcal{R}_0 > 1$, we choose a set of parameter values and compute the sensitivity indices of $\mathcal{R}_0$ with respect to each parameter, using the results to rank the above five intervention forms in order of significance.

3.1. Preliminary analysis

The five intervention forms are not all equal in the current degree of realisation: tracings, testings, and treatments —the so-called "3 Ts"— are reportedly suboptimal (Muthiariny & Murti, 2021), while vaccinations and social restrictions seem to be given primary attention (WHO Indonesia, 2022; COVID19 Vaccine Tracker; Afifa, 2022; Hutasoit, 2022). Accordingly, in this stage of our analysis, let us assume that the parameters u_3, u_4, and u_5, which represent the rates of the 3Ts, have fixed values. Furthermore, let us fix the values of all parameters except δ, u_1, and u_2.

As noted in section 1, $u_2 = 0$ represents normal mobility, while $u_2 = 1$ represents a total lockdown. The values of u_2 which represent social restrictions of level 1, 2, 3, and 4 can be estimated in the following way. First, we deal with level 1 social restrictions, which, as detailed in (Saptoyo & Kurniawan, 2021), consist of the following regulations:

(i) businesses in non-essential sectors are to implement the work-from-office policy at up to $p_1 = 75\%$ capacity;
(ii) businesses in essential sectors are to implement the work-from-office policy at up to $p_2 = 100\%$ capacity;
(iii) daily-need shops are to operate at up to $p_3 = 75\%$ capacity;
(iv) non-daily-need shops are to operate at up to $p_4 = 75\%$ capacity;
(v) malls and shopping centres are to operate at up to $p_5 = 75\%$ capacity;
(vi) roadside stalls and street vendors are to operate at up to $p_6 = 75\%$ capacity;
(vii) restaurants are to operate at up to $p_7 = 75\%$ capacity;
(viii) educational activities are to be carried out $p_8 = 50\%$ onsite and 50% online;
(ix) places of worship are to operate at up to $p_9 = 50\%$ capacity.

We estimate u_2 as the average percentage of restrictions in the case of level 1 social restrictions according to the above data: $u_2 = 1 - \left(\sum_{i=1}^{9} p_i\right)\Big/9 = 0.278$. In a similar way, we obtain the following values of u_2 representing social restrictions of level 2, 3, and 4: 0.389, 0.694, and 0.861, respectively. The values of δ, on the other hand, will be chosen in view of the efficacies of the actual COVID-19 vaccines (Globe, 2021; Jara et al., 2021; Mascellino, Timoteo, Angelis, & Oliva, 2021).

It is apparent from (5) and the definition of the k_is in (4) that, for any given δ, the graph of the equation $\mathcal{R}_0 = 1$ on the u_1u_2-plane is a straight line, the abscissa and ordinate intercepts being, respectively,

$$\ell_1 := \frac{\mu(\alpha\beta k_4\kappa\theta\lambda' + \alpha\beta\tau\theta\varphi\lambda' + \beta k_3k_4k_5\lambda\theta - k_1k_2k_3k_4k_5\mu)}{\alpha\beta\delta k_4\kappa\theta\lambda' + \alpha\beta\delta\tau\theta\varphi\lambda' + \beta\delta k_3k_4k_5\lambda\theta - \alpha\beta k_4\kappa\theta\lambda' - \alpha\beta\tau\theta\varphi\lambda' - \beta k_3k_4k_5\lambda\theta + k_1k_2k_3k_4k_5\mu}$$

and

$$\ell_2 := \frac{(\kappa\theta\beta\alpha\lambda' + k_3k_5(\beta\lambda\theta - k_1k_2\mu))k_4 + \alpha\beta\tau\theta\varphi\lambda'}{((\alpha\kappa\lambda' + k_3k_5\lambda)k_4 + \varphi\lambda'\tau\alpha)\beta\theta}.$$

Notice that ℓ_2 is independent of δ, since so are the k_is, by (4). Moreover, a direct computation shows that the denominator of ℓ_1 is equal to zero if and only if $\delta = \ell_2$. Furthermore, we let

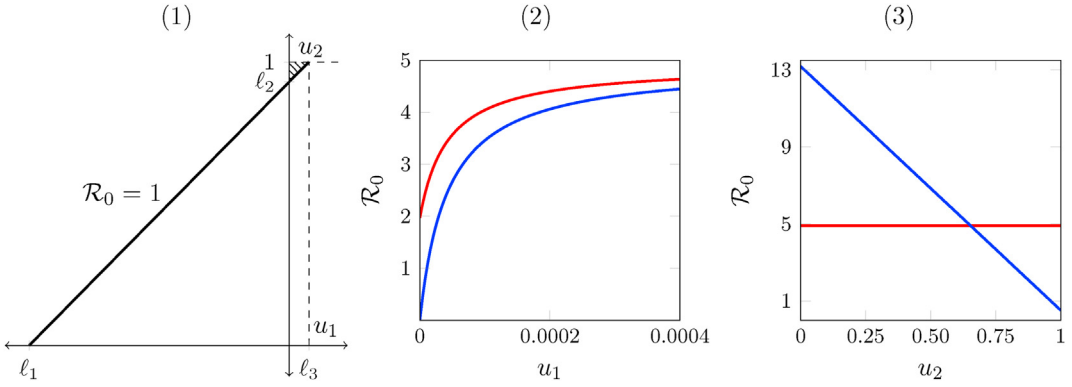

Fig. 2. (1) Plot of the line $\mathcal{R}_0 = 1$ on the u_1u_2-plane in the case of $\delta = 0.653$, with the feasible disease-free region shaded; (2) plot of $\mathcal{R}_0$ as a function of u_1 in the case of $\delta = 0.653$, for $u_2 = 0.861$ (red) and for $u_2 = 0.999995$ (blue); (3) plot of $\mathcal{R}_0$ as a function of u_2 in the case of $\delta = 0.653$, for $u_1 = 0.4$ (red) and for $u_1 = 0.000005$ (blue).

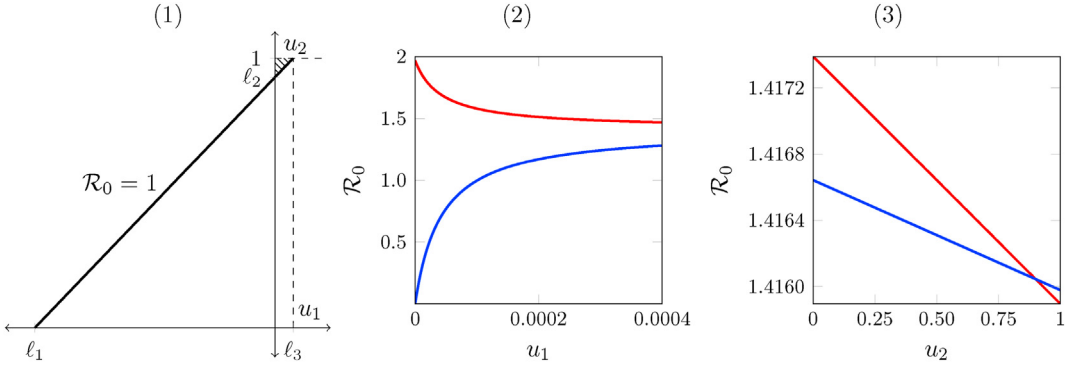

Fig. 3. (1) Plot of the line $\mathcal{R}_0 = 1$ on the u_1u_2-plane in the case of $\delta = 0.9$, with the feasible disease-free region shaded; (2) plot of $\mathcal{R}_0$ as a function of u_1 in the case of $\delta = 0.9$, for $u_2 = 0.861$ (red) and for $u_2 = 0.999995$ (blue); (3) plot of $\mathcal{R}_0$ as a function of u_2 in the case of $\delta = 0.9$, for $u_1 = 0.4$ (red) and for $u_1 = 0.9$ (blue).

$$\ell_3 := \frac{k_1k_2k_3k_4k_5\mu^2}{\alpha\beta k_4\kappa\theta\lambda' + \alpha\beta\tau\theta\varphi\lambda + \beta k_3k_4k_5\lambda\theta - k_1k_2k_3k_4k_5\mu - \alpha\beta\delta k_4\kappa\theta\lambda' - \alpha\beta\delta\tau\theta\varphi\lambda' - \beta\delta k_3k_4k_5\lambda\theta}$$

be the abscissa of the point of ordinate 1 on the line. Substituting the values shown in Table 1 of all parameters except δ, u_1, and u_2, one obtains

$$\begin{aligned}\ell_1 &= \frac{0.0000139049}{0.3549600264\delta - 0.3298930314},\\ \ell_2 &= 0.9293807942,\\ \ell_3 &= \frac{0.0000042150}{1.3160453862 - 1.4160453862\delta}.\end{aligned}$$

Recently, the vaccine most sought-after in the country is reportedly Sinovac's Coronavac (Bona, 2021), which has demonstrated a 65.3% efficacy (Globe, 2021; Jara et al., 2021). For this value of δ, we have $\ell_1 = -0.0001417358$ and $\ell_3 = 0.0000107698$, and the line $\mathcal{R}_0$ on the u_1u_2-plane is plotted in Fig. 2 (1). The shaded region is the feasible disease-free region, i.e., the region $\left\{(u_1, u_2) \in [0,1]^2 : \mathcal{R}_0 < 1\right\}$. Therefore, according to our model, using a vaccine with only a 65.3% efficacy, the pandemic can only be resolved if $u_1 \leqslant \ell_3 = 0.0000107698$, i.e., the vaccination rate is made extremely low, and $u_2 \geqslant \ell_2 = 0.9293807942$, i.e., a near-lockdown policy is implemented. The latter is uncompromisable: even level 4 social restrictions are insufficient; see the red curve in Fig. 2 (2). Likewise, if the vaccination rate is increased even only to a moderate level, say $u_1 = 0.4$ (Table 1), then the policy of raising the level of social restrictions becomes insignificant: such a policy suppresses the endemic-valued basic reproduction number —and thus the number of daily new cases— only insignificantly; see Fig. 2 (3). A major reason for this is that, for vaccinated citizens, social restrictions are waived,[4] allowing them to travel,

[4] Notice once again in the model's compartment diagram (Fig. 1) that the mobility restriction factor $1 - u_2$ is present in the transition rate from compartment S to compartment E, but not in the transition rate from compartment V to compartment E.

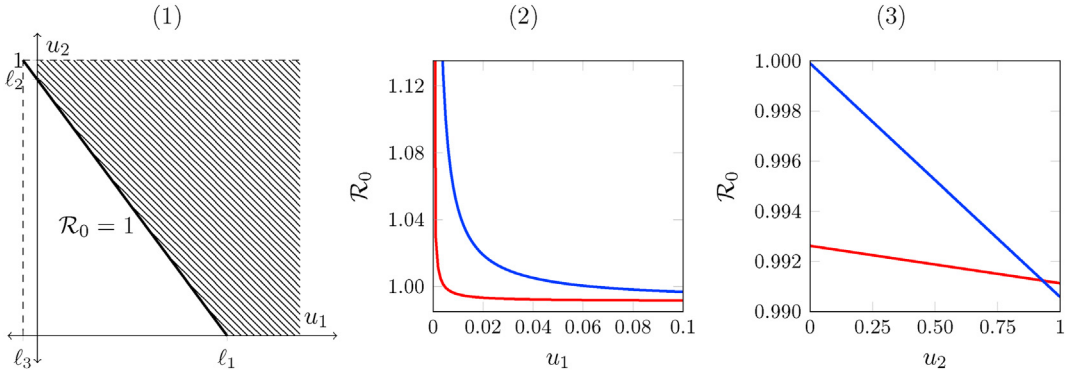

Fig. 4. (1) Plot of the line $\mathcal{R}_0 = 1$ on the u_1u_2-plane in the case of $\delta = 0.93$, with the feasible disease-free region shaded; (2) plot of $\mathcal{R}_0$ as a function of u_1 in the case of $\delta = 0.93$, for $u_2 = 0.861$ (red) and for $u_2 = 0$ (blue); (3) plot of $\mathcal{R}_0$ as a function of u_2 in the case of $\delta = 0.93$, for $u_1 = 0.4$ (red) and for $u_1 = 0.064$ (blue).

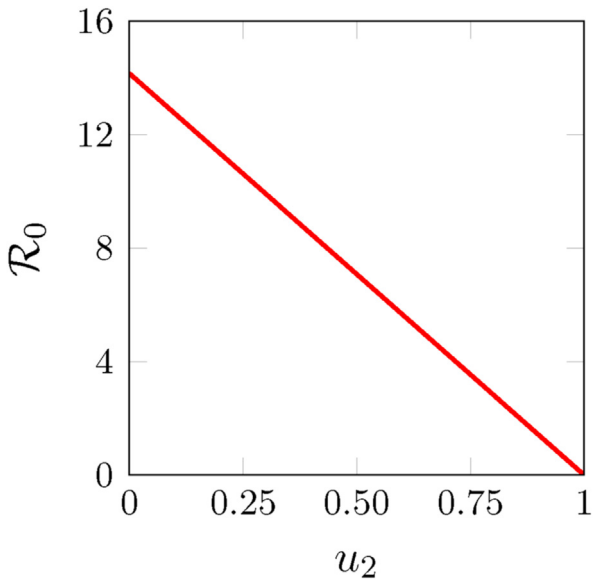

Fig. 5. Plot of $\mathcal{R}_0$ as a function of u_2 in the case of $u_1 = 0$.

visit public places, etc. more unrestrictedly than unvaccinated citizens, bringing about a high risk in the case of high vaccination rate but low vaccine efficacy. We thus find it unsurprising that the omicron wave remained unavoidable despite the notable progress of the country's vaccination programme (see section 1).

Now let us suppose that the country utilises a vaccine with a higher efficacy: say, $\delta = 0.9$. In this case, we have $\ell_1 = -0.0013332879$ and $\ell_3 = 0.0001013102$, and the line $\mathcal{R}_0$ on the u_1u_2-plane is plotted in Fig. 3 (1). Since no qualitative change is observed here, the message remains the same: the disease's transmission can only be halted with an extremely low vaccination rate and an extremely high level of mobility restrictions. However, comparing Fig. 2 (2) and Fig. 3 (2), we see a qualitative change: the red curve, which, in both figures, correspond to level 4 social restrictions, i.e., $u_1 = 0.861$, has changed monotonicity. Furthermore, comparing the quantitative properties of the red lines in Fig. 2 (3) and Fig. 3 (3), both corresponding to the moderate vaccination rate $u_1 = 0.4$, we can see that the improvement of the vaccine efficacy, from 0.653 to 0.9, drastically decreases the value of the basic reproduction number, from above 4 to below 2. We infer therefore that the improvement of the quality of COVID-19 vaccines should take precedence over that of the rate at which vaccinations are carried out.

Let us further increase the vaccine efficacy: $\delta = 0.93$. In this case, we have $\ell_1 = 0.0632634203$ and $\ell_3 = -0.0048070860$, and the line $\mathcal{R}_0$ on the u_1u_2-plane is plotted in Fig. 4 (1). Now, we see a radical qualitative change —a much desirable one— from Fig. 4 (1): the line's slope is now negative, and a disease-free state can be achieved even with a complete removal of social restrictions, i.e., $u_2 = 0$, and a very low vaccination rate, i.e., any low value of u_1 satisfying $u_1 \geqslant \ell_1 = 0.0632634203$, say, $u_1 = 0.064$ (i.e., 6.4% of the current number of susceptible individuals are vaccinated each day); see Fig. 4 (2) and (3).

A follow-up question naturally arises: is it possible to achieve a disease-free state without vaccinations, i.e., with $u_1 = 0$? In this case, the expression (5) for $\mathcal{R}_0$ is independent of δ:

$$\mathcal{R}_0 = \frac{(1-u_2)\beta(\alpha k_4 \kappa \lambda' + \alpha\tau\varphi\lambda' + k_3 k_4 k_5 \lambda)\theta}{\mu k_1 k_2 k_3 k_4 k_5} = 14.1604538645 - 14.1604538645 u_2;$$

a plot of $\mathcal{R}_0$ versus u_2 is shown in Fig. 5: a line with a negative slope which is rather large in absolute value. Therefore, in absence of vaccinations, raising the level of social restrictions suppresses the basic reproduction number significantly. This justifies the effectiveness of the government's social restriction policies prior to the commencement of the vaccination programme. Notice that, near $u_2 = 1$, the values of $\mathcal{R}_0$ shown Fig. 5 are lower than those shown in Fig. 2 (3). That is, in the cases where social restrictions are imposed on level 3 or 4, not administering vaccines results in lower values of $\mathcal{R}_0$ than administering vaccines with low efficacy, justifying that the assumed policy of waiving restrictions for vaccinated citizens is imprudent, since these citizens are not completely immune. Nevertheless, in absence of vaccinations, even level 4 social restrictions are not sufficient to bring the country to the disease-free state. The latter requires, again, a near-lockdown policy: $u_2 \geqslant \ell_2 = 0.9293807942$.

Let us summarise the recommended strategies arising from this first-stage analysis. Firstly, if a lockdown is undesirable, it is necessary to administer vaccinations. However, one should strive not primarily towards the increase of the rate at which they are administered, but towards the use of high-efficacy vaccines,[5] such as Pfizer-BioNTech or Moderna (Mascellino et al., 2021). Secondly, it is necessary to set out and implement an appropriate level of social restrictions to vaccinated citizens,[6] especially those who received vaccines with limited efficacy and/or have only been vaccinated partially.

3.2. Sensitivity analysis

Let us now complement the above analysis with a quantitative assessment of the significance of each parameter. We compute the *sensitivity index* (Chitnis, Hyman, & Cushing, 2008) of the basic reproduction number $\mathcal{R}_0$ with respect to a parameter p, i.e.,

$$\Upsilon_p^{\mathcal{R}_0} := \frac{\partial \mathcal{R}_0}{\partial p} \cdot \frac{p}{\mathcal{R}_0}, \tag{15}$$

for every $p \in \mathcal{P}$, where

$$\mathcal{P} := \{\lambda, \lambda', \mu, \mu', \beta, \delta, \alpha, \theta, \gamma, \varphi, \kappa, \tau, u_1, u_2, u_3, u_4, u_5\}$$

denotes the set of all parameters in the model (1), obtaining, e.g., for $p = \delta$ and $p = u_2$,

$$\Upsilon_\delta^{\mathcal{R}_0} = \frac{\delta u_1}{\delta u_1 + \mu u_2 - \mu - u_1} \qquad \text{and} \qquad \Upsilon_{u_2}^{\mathcal{R}_0} = \frac{\mu u_2}{\delta u_1 + \mu u_2 - \mu - u_1},$$

respectively.

We choose two sets of parameter values: one representing a disease-free case ($\mathcal{R}_0 < 1$), and another representing an endemic case ($\mathcal{R}_0 > 1$). In both sets, the values of $\lambda, \lambda', \mu, \mu', \beta, \alpha, \theta, \gamma, \varphi, \kappa, \tau, u_3, u_4, u_5$ are as shown in Table 1, and $\delta = 0.653$. In the former case, we set $(u_1, u_2) = \left(10^{-8}, 0.93\right)$, so that $\mathcal{R}_0 = 0.9921621498 < 1$, while in the latter, we set $(u_1, u_2) = (0.4, 0.278)$, so that $\mathcal{R}_0 = 4.9142369856 > 1$.

In each caese, we substitute the parameter values to all sensitivity indices. For each index $\Upsilon_p^{\mathcal{R}_0}$, the following aspects are essential.

1. The sign $sgn\left(\Upsilon_p^{\mathcal{R}_0}\right)$, which is positive (negative) if and only if $\mathcal{R}_0$ is monotonically increasing (decreasing) with p.
2. The absolute value $\Upsilon_p^{\mathcal{R}_0}$, which measures the relative change of $\mathcal{R}_0$ with respect to p: a $P\%$ change of p results in a $\left|\Upsilon_p^{\mathcal{R}_0}\right| P\%$ change of $\mathcal{R}_0$. Thus, the higher the value of $\left|\Upsilon_p^{\mathcal{R}_0}\right|$, the more significant the parameter p.

It was our intention to visualise the results using a bidirectional bar chart of the values of $\Upsilon_p^{\mathcal{R}_0}$ for every p in each case, but the rather unusual distribution of these values, especially in the disease-free case where an extreme outlier is present, makes such a chart ineffective.

For a more effective visualisation, let us first define the *significance rank* of a parameter p to be $r(p)$, where $r : \mathcal{P} \to \{1, \ldots, 17\}$ is the unique bijection for which

[5] The severity of the vaccines' side effects may also need to be considered for the acceptability of this strategy; alternatives include the utilisation of more than one type of vaccines with different levels of efficacy and side effects, the analysis of which requires a modification of the model (1); see section 4.

[6] This motivates another modification of the model (1); see section 4.

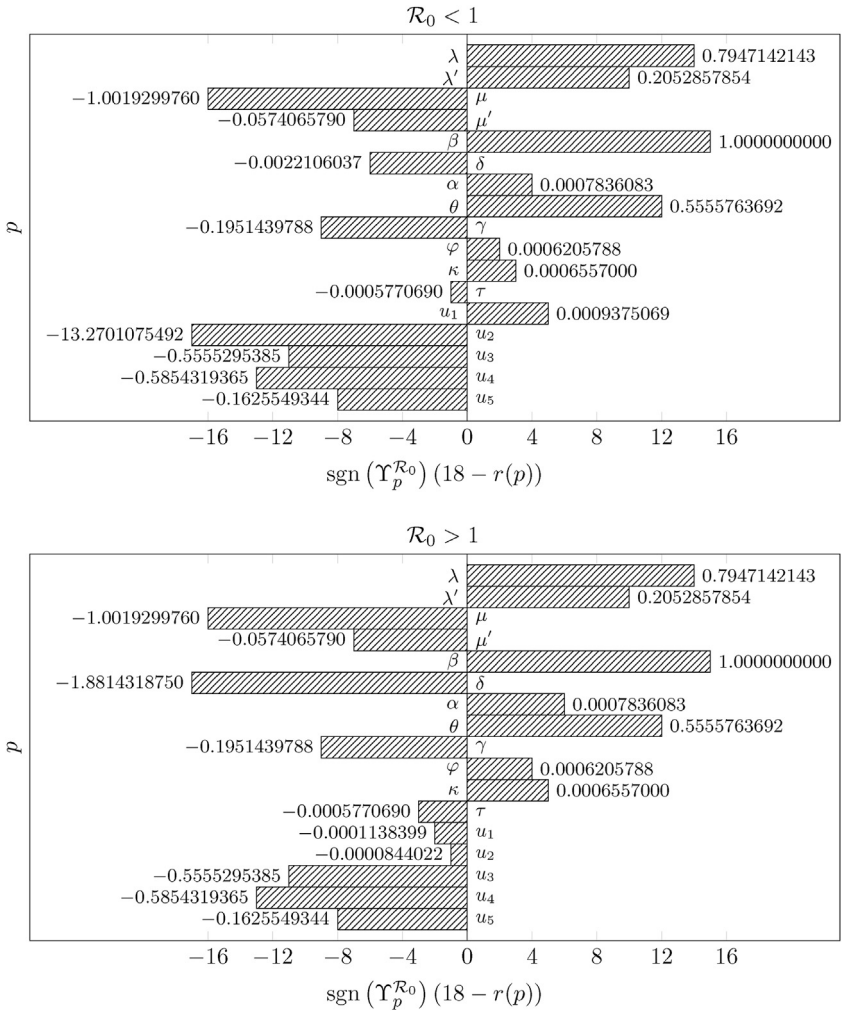

Fig. 6. Bidirectional bar charts, in which, for every parameter p, the value of $sgn\left(\Upsilon_p^{\mathcal{R}_0}\right)(18 - r(p))$ is represented by a bar which is labelled by the value of $\Upsilon_p^{\mathcal{R}_0}$, in the disease-free case (top) and endemic case (bottom) specified in subsection 3.2. Bars to the left (right) of the ordinate axis are associated with parameters with which the basic reproduction number is monotonically decreasing (increasing). The longer the bar, the more significant the associated parameter. Consequently, the ordering of the parameters according to significance in each case is given by (16) and (17).

$$\left|\Upsilon_{r^{-1}(1)}^{\mathcal{R}_0}\right| > \cdots > \left|\Upsilon_{r^{-1}(17)}^{\mathcal{R}_0}\right|.$$

Thus, the values of $18 - r(p)$ carry the same qualitative information as $\left|\Upsilon_p^{\mathcal{R}_0}\right|$: the higher the value of $18 - r(p)$, the more significant the parameter p. Therefore, instead of visualising the values of $\Upsilon_p^{\mathcal{R}_0} = sgn\left(\Upsilon_p^{\mathcal{R}_0}\right)\left|\Upsilon_p^{\mathcal{R}_0}\right|$, we visualise the values of $sgn\left(\Upsilon_p^{\mathcal{R}_0}\right)(18 - r(p))$, by bars which are labelled by the associated values of $\Upsilon_p^{\mathcal{R}_0}$ to retain the quantitative information (Fig. 6). We can see that the sequence of the parameters in decreasing order of significance is

$$\left(r^{-1}(n)\right)_{n=1}^{17} = (u_2, \mu, \beta, \lambda, u_4, \theta, u_3, \lambda', \gamma, u_5, \mu', \delta, u_1, \alpha, \kappa, \varphi, \tau) \tag{16}$$

in the disease-free case, and

$$\left(r^{-1}(n)\right)_{n=1}^{17} = (\delta, \mu, \beta, \lambda, u_4, \theta, u_3, \lambda', \gamma, u_5, \mu', \alpha, \kappa, \varphi, \tau, u_1, u_2) \tag{17}$$

in the endemic case. Let us now infer from these orderings the appropriate strategies of intervention in each case.

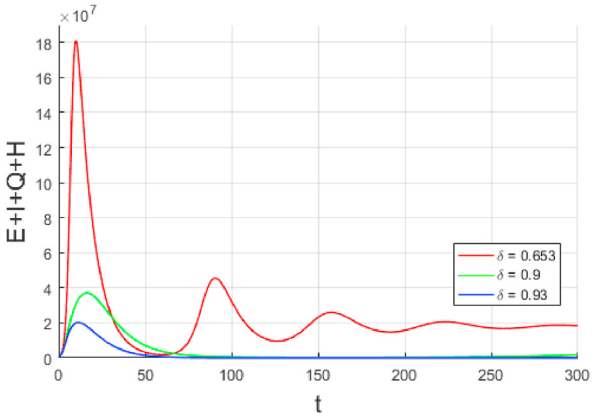

Fig. 7. Time-evolution of the number $E + I + Q + H$ of non-healthy individuals, for the parameter values shown in Table 1, $u_1 = 0.4$, and $u_2 = 0.278$, with $\delta = 0.653$ (red), $\delta = 0.9$ (green), and $\delta = 0.93$ (blue). Notice that, as δ is increased, both the maximum and the limit decrease drastically, showing the significance of δ. For $\delta = 0.93$, we observe convergence to the disease-free equilibrium.

3.2.1. The disease-free case

In the disease-free case, effort must be made in order to maintain the low value of the basic reproduction number. When the number of daily new cases rises, as the ordering (16) and Fig. 6 suggest, a committed implementation of social restrictions should be sufficient. Indeed, remarkably, tightening social restrictions only by 1% suppresses the basic reproduction number by 13.2701075492%. Other forms of intervention, if at all desired, are recommended in the following order: testings, tracings, treatments, and vaccinations. The latter is rather inessential, let alone when not supported by a high level of vaccine efficacy.

3.2.2. The endemic case

In the endemic case, significant effort is necessary for a transition to a disease-free state. The ordering (17) strongly supports our main finding in subsection 3.1: the vaccine efficacy being the parameter upon which the basic reproduction number depends most sensitively. Accordingly, we reiterate our primary finding in the previous subsection: that

1. raising the efficacy of vaccines

must be given the highest priority. With regards to the five forms of intervention, we recommend, in order of importance:

2. expanding and accelerating testings and tracings, so that infected and exposed individuals may be quarantined more immediately;
3. optimising treatments for infected individuals, by ensuring that health facilities and services (medications, hospital beds, medical practitioners, etc.) are in adequate availability;
4. administering vaccinations;
5. social restrictions, being the least important form of intervention, albeit, as previously remarked, may become significant if also applied to some degree to vaccinated individuals.

There is however a substantial difference in significance between recommendations (1) and (2)–(5), i.e., the rates of all five forms of intervention are far less significant than the vaccine efficacy. Indeed, increasing the vaccine efficacy from 65.3%, firstly to 90%, and subsequently to 93%, as narrated in subsection 3.1, results in significant drops of both the peak and limiting numbers of non-healthy individuals, the final value being sufficient for a transition from endemic to disease-free; see Fig. 7. On the other hand, assuming the original value of the vaccine efficacy, 65.3%, increasing any of the five intervention rates by 30%, or even by 60%, gives rise to barely any tangible impact; see Fig. 8. Therefore, the main key for a successful eradication of the pandemic is not a high rate of implementation of any of the five intervention forms, but a high-efficacy vaccine.

4. Conclusions and future research

We have constructed an SVEIQHR-type mathematical model for the spread of COVID-19, which incorporates as parameters the rates of the five forms of intervention presently realised by the government of Indonesia: vaccinations, social restrictions, tracings, testings, and treatments. We have computed the model's basic reproduction number $\mathcal{R}_0$, and show that the model possesses a unique disease-free equilibrium, which exists for all sets of parameter values and is stable (unstable) if $\mathcal{R}_0 < 1$ ($\mathcal{R}_0 > 1$), as well as a unique endemic equilibrium, which exists if $\mathcal{R}_0 > 1$.

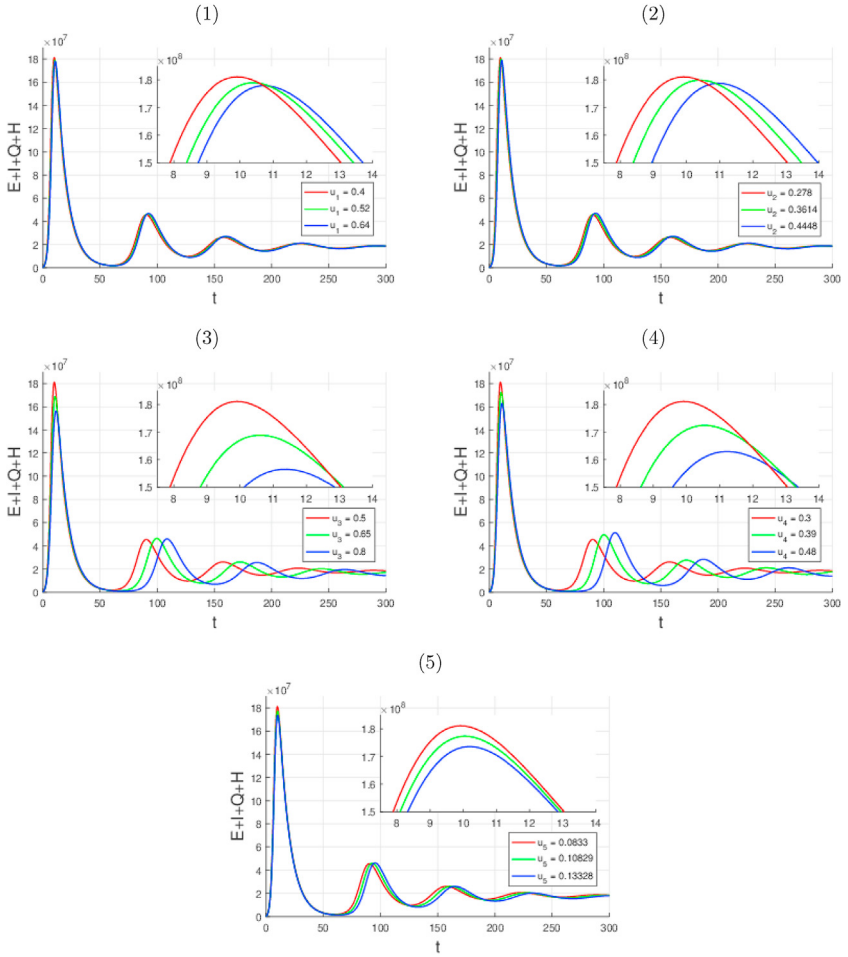

Fig. 8. Time-evolution of the number $E + I + Q + H$ of non-healthy individuals, for the parameter values shown in Table 1, $\delta = 0.653$, $u_1 = 0.4$, $u_2 = 0.278$, $u_3 = 0.5$, $u_4 = 0.3$, and $u_5 = 0.0833$ (red graphs on all panels), together with, on panel (i), where $i \in \{1, 2, 3, 4, 5\}$, the same in the cases of u_i being increased by 30% (green) and by 60% (blue). The magnifications near the maxima reflect the previously obtained order of importance of the intervention parameters: u_4, u_3, u_5, u_1, u_2. However, comparing with Fig. 7, we see that all these parameters are far less significant than δ.

We have also analysed the model numerically, with the aim of determining strategies by which the five intervention forms should be realised in order to optimise their impact. The analysis results in the following two major conclusions.

(1) In a disease-free state, social restrictions proved to be the best form of intervention in the case of a rise in the number of new cases.
(2) In an endemic state, a transition to disease-free state without vaccinations requires a near-lockdown policy. Since the country's government has refused to impose such a policy (Bulletin, 2021; Gorbiano & Sutrisno, 2020), vaccinations are necessary. However, efforts should be focused not primarily on increasing the vaccination rate (or even the rate of any other form of intervention), but on the use of vaccines with a high efficacy.

Finally, our model is open to further analysis. Indeed, one could continue the study of how the existence and local asymptotic stability of the model's endemic equilibria depend on its basic reproduction number, and investigate whether the equilibria's global (asymptotic) stability can be established using, e.g., Lyapunov functions (Korobeinikov, 2009; Melesse & Gumel, 2020; Safi & Gumel, 2010). Our model is also open to a number of modifications. One could incorporate a specified level of social restrictions for vaccinated individuals, and confirm whether, as a result, vaccination rate becomes more significant. Besides, the vaccinated compartment itself could be split into several compartments, in order to allow different assumptions on recipients of different vaccines and/or, in the case of multi-dose vaccines, recipients of different numbers of vaccine doses. Similarly, the quarantined compartment could be split into several compartments, in order to distinguish the isolated individuals (i.e., the separated infected individuals) from the quarantined individuals (i.e., the separated exposed individuals) —which may further be split according to their vaccination histories— so that different recovery rates and/or

time-delays may be employed. Finally, one could devote more explicit attention to a new virus variant by splitting the infected compartment into that of individuals infected by the new variant and that of those infected otherwise.

Declaration of interests

The authors declare that they have no known competing financial interests or personal relationships that could have appeared to influence the work reported in this paper.

Acknowledgements

This research was supported by Parahyangan Catholic University via the Publikasi Internasional Bereputasi research grant scheme 2022 (Number: III/LPPM/2022-02/75-P).

References

Adjie, M. F. P. (May 16, 2020). Let's coexist with COVID-19': Jokowi calls on residents to adapt to 'new normal. *The Jakarta Post* https://www.thejakartapost.com/news/2020/05/16/lets-coexist-with-covid-19-jokowi-calls-on-residents-to-adapt-to-new-normal.html.

Afifa, L. (January 18, 2022). *Jokowi urges Indonesians to get booster shots*. Tempo.co. https://en.tempo.co/read/1551390/jokowi-urges-indonesians-to-get-booster-shots.

Albani, V. V. L., Loria, J., Massad, E., & Zubelli, J. P. (2021a). COVID-19 underreporting and its impact on vaccination strategies. *BMC Infectious Diseases, 21*, 1111.

Albani, V. V. L., Loria, J., Massad, E., & Zubelli, J. P. (2021b). The impact of COVID-19 vaccination delay: A data-driven modeling analysis for Chicago and New York city. *Vaccine, 39*, 6088–6094.

Albani, V. V. L., Velho, R. M., & Zubelli, J. P. (2021c). Estimating, monitoring, and forecasting COVID-19 epidemics: A spatiotemporal approach applied to NYC data. *Scientific Reports, 11*, 9089.

Aldila, D., Khoshnaw, S. H. A., Safitri, E., Anwar, Y. R., Bakry, A. R. Q., Samiadji, B. M., et al. (2020a). A mathematical study on the spread of COVID-19 considering social distancing and rapid assessment: The case of Jakarta, Indonesia. *Chaos, Solitons & Fractals, 139*, Article 110042.

Aldila, D., Ndii, M. Z., & Samiadji, B. M. (2020b). Optimal control on COVID-19 eradication program in Indonesia under the effect of community awareness. *Mathematical Biosciences and Engineering, 17*, 6355–6389.

Aldila, D., Samiadji, B. M., Simorangkir, G. M., Khosnaw, S. H. A., & Shahzad, M. (2021). Impact of early detection and vaccination strategy in COVID-19 eradication program in Jakarta, Indonesia. *BMC Research Notes, 14*, 1–7.

Alharbi, Y., Alqahtani, A., Albalawi, O., & Bakouri, M. (2020). Epidemiological modeling of COVID-19 in Saudi Arabia: Spread projection, awareness, and impact of treatment. *Applied Sciences* (Vol. 2020,, 5895.

Allen, L. J. S. (2007). *An introduction to mathematical Biology*. New Jersey: Pearson Prentice Hall.

Amaku, M., Covas, D. T., Coutinhbo, F. A. B., Neto, R. S. A., Struchiner, C., Wilder-Smith, A., et al. (2021b). Modelling the test, trace and quarantine strategy to control the COVID-19 epidemic in the state of São Paulo, Brazil. *Infectious Disease Modelling, 6*, 46–55.

Amaku, M., Covas, D. T., Coutinho, F. A. B., Azevedo, R. S., & Massad, E. (2021a). Modelling the impact of delaying vaccination against SARS-CoV-2 assuming unlimited vaccine supply. *Theoretical Biology and Medical Modelling, 18*, 1–11.

Arief, I., Adji, R., & Suharto. (December 13, 2021). *Govt to push booster vaccinations starting jan 2022: Official*. ANTARA News. https://en.antaranews.com/news/204329/govt-to-push-booster-vaccinations-starting-jan-2022-official.

Aronnaa, M. S., Guglielmi, R., & Moschen, L. M. (2021). A model for COVID-19 with isolation, quarantine and testing as control measures. *Epidemics, 34*, Article 100437.

Babaei, A., Jafari, H., Banihashemi, S., & Ahmadi, M. (2021). Mathematical analysis of a stochastic model for spread of coronavirus. *Chaos, Solitons & Fractals, 145*, Article 110788.

Bona, M. F. (December 5, 2021). *Sinovac becomes Indonesia's most sought-after vaccine*. Jakarta Globe. https://jakartaglobe.id/news/sinovac-becomes-indonesias-most-soughtafter-vaccine.

Bubar, K. M., Reinholt, K., Kissler, S. M., Lipsitch, M., Cobey, S., Grad, Y. H., et al. (2021). Model-informed COVID-19 vaccine prioritization strategies by age and serostatus. *Science, 371*, 916–921.

Bulletin, B.orneo (June 25, 2021). Jokowi refuses to lock down as Indonesia's daily cases soar past 15,000. *Borneo Bulletin*. https://borneobulletin.com.bn/jokowi-refuses-to-lock-down-as-indonesias-daily-cases-soar-past-15000/.

Calvetti, D., Hoover, A. P., Rose, J., & Somersalo, E. (2020). Metapopulation network models for understanding, predicting, and managing the coronavirus disease COVID-19. *Frontiers in Physics, 8*, 261.

Chen, Y. H., Fang, C. T., & Huang, Y. L. (2021). Effect of non-lockdown social distancing and testing-contact tracing during a COVID-19 outbreak in Daegu, South Korea, February to April 2020: A modeling study. *International Journal of Infectious Diseases, 110*, 213–221.

Chitnis, N., Hyman, J. M., & Cushing, J. M. (2008). Determining important parameters in the spread of malaria through the sensitivity analysis of a mathematical model. *Bulletin of Mathematical Biology, 70*, 1272–1296.

Choi, S., & Ki, M. (2020). Analyzing the effects of social distancing on the COVID-19 pandemic in Korea using mathematical modeling. *Epidemiology and Health, 42*, Article e2020064.

COVID19 Vaccine Tracker, 11 vaccines approved for use in Indonesia. https://covid19.trackvaccines.org/country/indonesia/.

Cui, Y., Ni, S., & Shen, S. (2021). A network-based model to explore the role of testing in the epidemiological control of the COVID-19 pandemic. *BMC Infectious Diseases, 21*, 1–12.

Dashtbali, M., & Mirzaie, M. (2021). A compartmental model that predicts the effect of social distancing and vaccination on controlling COVID-19. *Scientific Reports, 11*, 1–11.

Departemen Dalam Negeri. (2021a). *Instruksi Menteri Dalam Negeri No. 42 Tahun 2021 tentang Pemberlakuan Pembatasan Kegiatan Masyarakat level 4, level 3, dan level 2 Corona virus disease 2019 di Wilayah Jawa dan Bali*. Jakarta: Kementerian Dalam Negeri. https://covid19.go.id/storage/app/media/Regulasi/2021/September/salinan-inmendagri-no-42-tahun-2021-tentang-ppkm-level-4-level-3-dan-level-2-covid-2019-di-wilayah-jawa-dan-bali.pdf.

Departemen Dalam Negeri. (2021b). *Instruksi Menteri Dalam Negeri No. 47 Tahun 2021 tentang Pemberlakuan Pembatasan Kegiatan Masyarakat level 4, level 3, level 2, dan level 1 Corona virus disease 2019 di Wilayah Jawa dan Bali*. Jakarta: Kementerian Dalam Negeri. https://covid19.go.id/storage/app/media/Regulasi/2021/Oktober/salinan-inmendagri-no-47-tahun-2021-tentang-ppkm-level-4-level-3-level-2-dan-level-1-covid-19-di-jawa-bali.pdf.

News Desk. (October 12, 2020). *Rapid antigen tests 'alternative' but PCR tests remain key to handling pandemic*. Eijkman Institute. *The Jakarta Post* https://www.thejakartapost.com/news/2020/10/11/rapid-antigen-tests-alternative-but-pcr-tests-remain-key-to-handling-pandemic-eijkman-institute.html.

Diagne, M. L., Rwezaura, H., Tchoumi, S. Y., & Tchuenche, J. M. (2021). A mathematical model of COVID-19 with vaccination and treatment. *Computational and Mathematical Methods in Medicine*, 2021.

Double, M.. The new policy of PPKM level 1 to 4. https://www.double-m.co/en/the-new-policy-of-ppkm-level-1-to-4/.

van den Driessche, P., & Watmough, J. (2002). Reproduction numbers and sub-threshold endemic equilibria for compartmental models of disease transmission. *Mathematical Biosciences, 180*, 29–48.

Indonesia Expat. (2022). New quarantine rules for Indonesians returning confirmed. *Indonesia Expat, 2*. January https://indonesiaexpat.id/news/new-quarantine-rules-for-indonesians-returning-confirmed/.
Ferguson, N. M., Laydon, D., Nedjati-Gilani, G., Imai, N., Ainslie, K., Baguelin, M., et al. (2020). *Report 9: Impact of non-pharmaceutical interventions (NPIs) to reduce COVID-19 mortality and healthcare demand*. Imperial College London.
Gatto, N. M., & Schellhorn, H. (2021). Optimal control of the SIR model in the presence of transmission and treatment uncertainty. *Mathematical Biosciences, 333*, Article 108539.
Gibbons, C. L., Mangen, M. J., Plass, D., Havelaar, A. H., Brooke, R. J., Kramarz, P., et al. (2014). Measuring underreporting and under-ascertainment in infectious disease datasets: A comparison of methods. *BMC Public Health, 14*, 147.
Jakarta Globe. (2021). Indonesia approves Sinovac vaccine amid dramatic surge in coronavirus cases. *Jakarta Globe, January, 11*. https://jakartaglobe.id/news/indonesia-approves-sinovac-vaccine-amid-dramatic-surge-in-coronavirus-cases.
Gorbiano, M. I., & Sutrisno, B. (March 30, 2020). Jokowi refuses to impose lockdown on Jakarta. *Jakarta Post*. https://www.thejakartapost.com/news/2020/03/30/jokowi-refuses-to-impose-lockdown-on-jakarta.html.
Grimm, V., Mengel, F., & Schimdt, M. (2021). Extensions of the SEIR model for the analysis of tailored social distancing and tracing approaches to cope with COVID-19. *Scientific Reports, 11*, 4214.
Gugus Tugas Percepatan Penanganan COVID-19, Peta sebaran. Covid19.go.id https://covid19.go.id/peta-sebaran.
Hutasoit, M. (January 10, 2022). BRIN researchers remind about contact tracing ability to face omicron variants. *VOI*. https://voi.id/en/news/122588/brin-researchers-remind-about-contact-tracing-ability-to-face-omicron-variants.
Indonesia Expat, 3,000 people enter Indonesia from overseas every day. *Indonesia Expat*, (December 18, 2021). https://indonesiaexpat.id/news/3000-people-enter-indonesia-from-overseas-every-day/.
Jara, A., Undurraga, E. A., González, C., Paredes, F., Fontecilla, T., Jara, G., et al. (2021). Effectiveness of an inactivated SARS-CoV-2 vaccine in Chile. *New England Journal of Medicine, 385*, 875–884.
Junida, A. I., Ihsan, N., & Suharto. (March 7, 2022). Vaccinated travelers no longer obliged to present COVID-19 test report. *ANTARA News*. https://en.antaranews.com/news/218637/vaccinated-travelers-no-longer-obliged-to-present-covid-19-test-report.
Korobeinikov, A. (2009). Global properties of SIR and SEIR epidemic models with multiple parallel infectious stages. *Bulletin of Mathematical Biology, 71*, 75–83.
Lau, H., Khosrawipour, T., Kocbach, P., Ichii, H., Bania, J., & Khosrawipour, V. (2021). Evaluating the massive underreporting and undertesting of COVID-19 cases in multiple global epicenters. *Pulmonology, 27*, 110–115.
LimaCampos, E., Cysne, R. P., Madureira, A. L., & Mendes, G. L. Q. (2021). Multi-generational SIR modeling: Determination of parameters, epidemiological forecasting and age-dependent vaccination policies. *Infectious Disease Modelling, 6*, 751–765.
Martcheva, M. (2015). *An introduction to mathematical epidemiology*. New York: Springer.
Mascellino, M. T., Timoteo, F. D., Angelis, M. D., & Oliva, A. (2021). Overview of the main anti-SARS-CoV-2 vaccines: Mechanism of action, efficacy and safety. *Infection and Drug Resistance, 14*, 3459–3476.
Melesse, D. Y., & Gumel, A. B. (2020). Global asymptotic properties of an SEIRS model with multiple infectious stages. *Journal of Mathematical Analysis and Applications, 366*, 202–217.
Menteri Kesehatan Republik Indonesia, Keputusan Menteri Kesehatan Republik Indonesia Nomor HK.01.07/MENKES/4805/2021.(2021). Jakarta https://covid19.hukumonline.com/wp-content/uploads/2021/08/keputusan_menteri_kesehatan_nomor_hk_01_07_menkes_4805_2021_tahun_2021.pdf.
Moghadas, S. M., Vilches, T. N., Zhang, K., Wells, C. R., Shoukat, A., Singer, B. H., et al. (2021). The impact of vaccination on coronavirus disease 2019 (COVID-19) outbreaks in the United States. *Clinical Infectious Diseases, 73*, 2257–2264.
Muñoz-Fernández, G. A., Seoane, J. M., & Seoane-Sepúlveda, J. B. (2021). A SIR-type model describing the successive waves of COVID-19. *Chaos, Solitons & Fractals, 144*, Article 110682.
Muthiariny, D. E., & Murti, M. W. (March 1, 2021). *Indonesia needs two more years to fight COVID-19: Epidemiologist*. Tempo.co. https://en.tempo.co/read/1437726/indonesia-needs-two-more-years-to-fight-covid-19-epidemiologist.
Mwalili, S., Kimathi, M., Ojiambo, V., Gathungu, D., & Mbogo, R. (2020). SEIR model for COVID-19 dynamics incorporating the environment and social distancing. *BMC Research Notes, 13*, 352.
Page, M. L. (2021). The omicron wave. *New Scientist, 252*, 7.
Prem, K., Liu, Y., Russell, T. W., Kucharski, A. J., Eggo, R. M., Davies, N., et al. (2020). The effect of control strategies to reduce social mixing on outcomes of the COVID-19 epidemic in Wuhan, China: A modelling study. *The Lancet Public Health, 5*, e261–e270.
Ranggasari, R., & Bhwana, P. G. (December 21, 2021). *3 omicron cases in Indonesia with traces to 250 close contacts; 10 infections*. Tempo.co. https://en.tempo.co/read/1541657/3-omicron-cases-in-indonesia-with-traces-to-250-close-contacts-10-infections.
Rayda, N. (February 2, 2022). *Record high of more than 57,000 new COVID-19 cases in Indonesia*. Channel News Asia. https://www.channelnewsasia.com/asia/indonesia-record-high-covid-19-cases-omicron-2499771.
Robinson, R. C. (2012). *An introduction to dynamical systems: Continuous and discrete* (2nd ed.). Rhode Island: American Mathematical Society.
Saberi, M., Hamedmoghadam, H., Madani, K., Dolk, H. M., Morgan, A. S., Morris, J. K., et al. (2020). Accounting for underreporting in mathematical modeling of transmission and control of COVID-19 in Iran. *Frontiers in Physics, 8*, 289.
Sadarangani, M., Raya, B. A., Conway, J. M., Iyaniwura, S. A., Falcao, R. C., Colijn, C., et al. (2021). Importance of COVID-19 vaccine efficacy in older age groups. *Vaccine, 39*, 2020–2023.
Safi, M. A., & Gumel, A. B. (2010). Global asymptotic dynamics of a model for quarantine and isolation. *Discrete andd Continuous Dynamical Systems B, 14*, 209.
Saptoyo, R. D. A., & Kurniawan, R. F. (July 31, 2021). *Ini perbedaan aturan PPKM level 1, 2, 3 dan 4*. Kompas.com. https://www.kompas.com/tren/read/2021/07/31/150000165/ini-perbedaan-aturan-ppkm-level-1-2-3-dan-4.
Saxena, S. K. (2020). *Coronavirus disease 2019 (COVID-19)*. Singapore: Springer.
Shakhany, M. Q., & Salimifard, K. (2021). Predicting the dynamical behavior of COVID-19 epidemic and the effect of control strategies. *Chaos, Solitons & Fractals, 146*, Article 110823.
Shofa, J. N. (2022b). Gov't secures 400,000 molnupiravir tablets as omicron cases rise. *Jakarta Globe, January, 19*. https://jakartaglobe.id/news/govt-secures-400000-molnupiravir-tablets-as-omicron-cases-rise.
Shofa, J. N. (February 16, 2022). *Despite case surge, bed occupancy rate remains low: gov't*. Jakarta Globe. https://jakartaglobe.id/news/despite-case-surge-bed-occupancy-rate-remains-low-govt.
Sucipto, T. I. (February 7, 2022). Govt raises PPKM status in Greater Jakarta to level 3. *Medcom.id*. https://www.medcom.id/english/national/8N0GMzEK-govt-raises-ppkm-status-in-greater-jakarta-to-level-3.
Syakriah, A. (January 11, 2021). Over 132 million Indonesians fully vaccinated against COVID-19, *the Jakarta Post*. https://www.thejakartapost.com/news/2021/01/11/indonesia-allows-emergency-use-of-sinovac-vaccine.html.
Triwadani, R. (2021). Indonesian officials and media fight vaccine hesitancy, misinformation. *Asian Politics & Policy, 13*, 635–639.
WHO. (February 1, 2021). *Contact tracing in the context of COVID-19: Interim guidance*. World Health Organization. https://apps.who.int/iris/bitstream/handle/10665/339128/WHO-2019-nCoV-Contact_Tracing-2021.1-eng.pdf.
WHO. (February 8, 2022). *COVID-19 weekly epidemiological update (edition 78*. World Health Organization. https://www.who.int/docs/default-source/coronaviruse/situation-reports/20220208_weekly_epi_update_78.pdf.
WHO Indonesia, coronavirus disease 2019 (COVID-19): Situation report 17, World health Organization Indonesia.(July 22, 2020). https://cdn.who.int/media/docs/default-source/searo/indonesia/covid19/external-situation-report-17-21july2020.pdf.
WHO Indonesia, coronavirus disease 2019 (COVID-19): Situation report 60, *World health Organization Indonesia*. https://cdn.who.int/media/docs/default-source/searo/indonesia/covid19/external-situation-report-60_23-june-2021.pdf, (June 23, 2021).

WHO Indonesia, coronavirus disease 2019 (COVID-19): Situation report 86, *World health Organization Indonesia*. https://cdn.who.int/media/docs/default-source/searo/indonesia/covid19/external-situation-report-86_19-january-2022.pdf, (January 19, 2022).
Wolf, C., Matthews, A. L., & Alas, H. (February 23, 2022). *COVID-19 vaccination gulf widens between wealthy, developing countries*. US News. https://www.usnews.com/news/best-countries/articles/covid-19-vaccination-rates-by-country.
The World Bank. (2020). *Population, total - Indonesia*. https://data.worldbank.org/indicator/SP.POP.TOTL?locations=ID.
Yong, B., Hoseana, J., & Owen, L. (2022b). A design of governmental policies for the eradication of COVID-19 in Jakarta using an SIR-type mathematical model. *Communications in Mathematical Biology and Neuroscience, 2022*. Article ID 26.
Yong, B., Owen, L., & Hoseana, J. (2022a). Mathematical analysis of an epidemic model for COVID-19: How important is the people's cautiousness level for eradication? *Letters in Biomathematics, 9*, 3–22.